# Phthalein Derivatives as a New Tool for Selectivity in Thymidylate Synthase Inhibition

Paola M. Costi,*,† Marcella Rinaldi,† Donatella Tondi,† Piergiorgio Pecorari,† Daniela Barlocco,*,‡ Stefano Ghelli,§ Robert M. Stroud,⊥ Daniel V. Santi,⊥ Thomas J. Stout,⊥ Chiara Musiu,∥ Elena M. Marangiu,∥ Alessandra Pani,∥ Donatella Congiu,∥ Giulia A. Loi,∥ and Paolo La Colla*,∥

*Dipartimento Scienze Farmaceutiche and Dipartimento Scienze Chimiche, Università di Modena e Reggio Emilia, Via Campi 183, 41100 Modena, Italy, Istituto Chimica Farmacologia e Tossacologia, Università Milano, Viale Abruzzi 42, 20131 Milano, Italy, Departments of Biochemistry and Biophysics and of Pharmaceutical Chemistry, University of California, San Francisco, California 94143, and Dipartimento Biologia Sperimentale, Università di Cagliari, v.le Regina Margherita 45, 09214 Cagliari, Italy*

*Received January 4, 1999*

A new set of phthalein derivatives stemming from the lead compound, phenolphthalein, were designed to specifically complement structural features of a bacterial form of thymidylate synthase (*Lactobacillus casei*, LcTS) versus the human TS (hTS) enzyme. The new compounds were screened for their activity and their specificity against TS enzymes from different species, namely, *L. casei* (LcTS), *Pneumocystis carinii* (PcTS), *Cryptococcus neoformans* (CnTS), and human thymidylate synthase (hTS). Apparent inhibition constants ($K_i$) for all the compounds against LcTS were determined, and inhibition factors (IF, ratio between the initial rates of the enzymatic reaction in the presence and absence of each inhibitor) against each of the four TS species were measured. A strong correlation was found between the two activity parameters, IF and $K_i$, and therefore the simpler IF was used as a screening factor in order to accelerate biological evaluation. Compounds **5b**, **5c**, **5ba**, and **6bc** showed substantial inhibition of LcTS while remaining largely inactive against hTS, illustrating for the first time remarkable species specificity among TSs. Due to sequence homology between the enzymes, several compounds also showed high activity and specificity for CnTS. In particular, 3-hydroxy-3-(3-chloro-4-hydroxyphenyl)-6-nitro-1*H*,3*H*-naphtho[1,8-*c*,*d*]pyran-1-one (**6bc**) showed an IF < 0.04 for CnTS ($K_i$ = 0.45 $\mu$M) while remaining inactive in the hTS assay at the maximum solubility concentration of the compound (200 $\mu$M). In cell culture assays most of the compounds were found to be noncytotoxic to human cell lines but were cytotoxic against several species of Gram-positive bacteria. These results are consistent with the enzymatic assays. Intriguingly, several compounds also had selective activity against *Cr. neoformans* in cell culture assay. In general, the most active and selective compounds against the Gram-positive bacteria were those designed and found in the enzyme assay to be specific for LcTS versus hTS. The original lead compound was least selective against most of the cell lines tested. To our knowledge these compounds are the first TS inhibitors selective for bacterial TS with respect to hTS.

## Introduction

Thymidylate synthase (TS), an enzyme crucial to DNA synthesis in both prokaryotic and eukaryotic cells, is a target for the development of antibacterial, antimycotic, anticancer, and recently, antiviral agents.[1−3] TS catalyzes the conversion of deoxyuridine monophosphate (dUMP) to deoxythymidine monophosphate (dTMP) by a reductive methylation involving $N^5$,$N^{10}$-methylenetetrahydrofolate (mTHF) as a cofactor.[4] In the absence of the additional formation of dTMP via thymidine kinase (salvage pathway), the reaction catalyzed by TS is the rate-limiting step in DNA synthesis since it is the sole de novo pathway for the synthesis of dTTP (deoxythymidine triphosphate). Therefore, inhibition of TS would prevent cell multiplication. The primary structure of TS from various sources has been assessed.[5] In some cases, crystal structures of apoenzymes and/or of binary and ternary TS complexes with substrates and/or ligands have also been solved.[6−12] In particular, the structures of the enzymes from *Lactobacillus casei*, *Escherichia coli, Pneumocystis carinii*,[6,9,10] and, more recently, human cells have been reported.[12] These studies give information on the enzyme's structure and function, on the binding sites, and on the modes of binding of different TS inhibitors, thus providing the setting for structure-based drug design.[13,14] Several TS inhibitors able to bind either at the pyrimidine substrate or at the folate cofactor sites, most of which have been developed as anticancer agents, are known.[1] The classical folate analogues, such as CB3717, and especially the more recent ones, such as BW1843U89 (Figure 1), are very potent inhibitors of human TS.[15−23] They are powerful antitumor agents with acknowledged adverse side effects. Some problems are related to their metabolic pathway:[24,25] they require a carrier (reduced folate

* To whom correspondence should be addressed.
† Dipartimento Scienze Chimiche, Università di Modena e Reggio Emilia.
‡ Università Milano.
§ Dipartimento Scienze Farmaceutiche, Università di Modena e Reggio Emilia.
⊥ University of California.
∥ Universita di Cagliari.

10.1021/jm9900016 CCC: $18.00 
Published on Web 05/29/1999

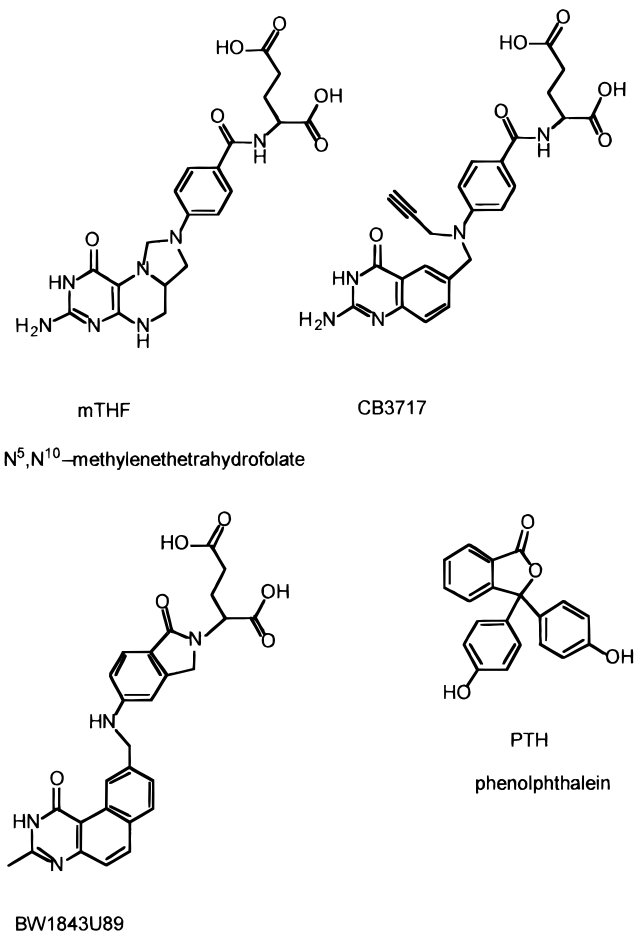


**Figure 1.** Folate cofactor and TS antifolates.

carrier, RFC) to carry a prodrug thorough the cell membrane and enter the cells, where they subsequently need to be activated to produce a more effective inhibitor of the enzyme. These prodrugs are substrates of folylpolyglutamyl synthetase (FPGS), which attaches additional glutamic acid residues to the one already present.[24,25] The resulting polyglutamylated form often binds more tightly to TS than the monoglutamylated form. Moreover, these compounds bind in nearly the same mode as the natural folate cofactor.[19] This site is well-conserved in both the primary and the tertiary structures among TS enzymes from different species. This could explain why no selectivity has been obtained to date: compounds that inhibit eukaryotic TS usually also inhibit the prokaryotic enzyme.

To our knowledge, the potential capability of a compound to bind bacterial TS with higher affinity than the human enzyme has not been deeply investigated.[19,21,26] In most cases, compounds designed to be selective have failed.[19,20] In principle, the knowledge of structural details of enzymes from different organisms presents the opportunity to rationally design new compounds exploiting the structural differences existing in the active sites of the different species.

Starting from the X-ray crystal structure of the complex of the novel inhibitor phenolphthalein (PTH, **1a**) (Figure 2), bound to LcTS,[26] new compounds were designed and synthesized. These phthalein analogues were designed to take advantage of differences in structural aspects of the bacterial active site not found in the human enzyme. Several of these derivatives had considerable specificity for LcTS versus hTS and also showed selective toxicity in bacterial versus human cell line culture assays.

The present paper deals with the design, the synthesis, the characterization, and the biological evaluation of compounds designed to be selective against bacterial TS (obtained from the Gram-positive organism *L. casei*) and not against hTS. To our knowledge these are the first inhibitors of TS to show such species selectivity. The bases for structural recognition of the phthalein analogues are discussed; detailed analysis of the mode of binding through computational chemistry and mutagenesis will be described elsewhere.[27]

## Design

The crystal structure of the phenolphthalein−LcTS complex has been solved at 2.3 Å resolution.[26] Phenolphthalein is found to occupy the top of the folate binding site (Figure 2). The ligand makes hydrogen bonds with Asp221, Glu60, and Arg23. In particular, one phenol hydroxyl group makes a hydrogen bond with Glu60 through a conserved water molecule (Wat404), while the other hydroxyl group makes a hydrogen bond with Asp221 (*L. casei* numbering) ($O_\delta$1 2.95 Å). The carbonyl of phenolphthalein is directed toward the −NH of Arg23 (at a distance of 4.02 Å). The phthalidic ring points toward the large empty space present in the folate pocket and does not interact directly with any other residue. Specifically, position 4 of the phthalidic benzene ring is 3.54 Å from Trp85. Positions 5 and 6 are 4.21 and 4.25 Å from Glu84, respectively, while position 7 points completely out of the folate site. The orientation of the phthalidic ring points toward a previously unexplored region of the active site. Specifically, the benzene ring approaches residues ordinarily uninvolved in ligand binding: Val314 (4.58 Å), Ile81 (5.80 Å), and Ala194 (7.7 Å).

On the basis of this novel ligand-binding mode, we designed a new series of phthalein analogues with an expanded phthalidic ring. This ring expansion was intended to bridge the empty space found in the PTH complex and make novel interactions with distal residues which are specific to bacterial forms of TS. On the basis of graphical modeling, the new 1,8-naphthalidic derivative appeared to fit well into the binding pocket, substantially maintaining its binding mode with respect to phenolphthalein. The phenolic rings of the 1,8-naphthalidic derivative superimposed well with those of phenolphthalein. Modeling also indicated that introduction of halogen substituents at the ortho-position on the phenol ring would not cause large steric clashes, would improve the binding energy with additional interactions, and would influence the hydrogen bond strength of the phenolic function.

## Chemistry

The syntheses of compounds **1** and **2** from phthalic or 2,3-naphthalic anhydride, respectively, are depicted in Scheme 1. Accordingly, heating the required anhydride at 180 °C for 5 h with the appropriate (substituted) phenol in the presence of a few drops of sulfuric acid gave the desired phthaleins, which were subsequently purified by silica gel chromatography (Table 1). The

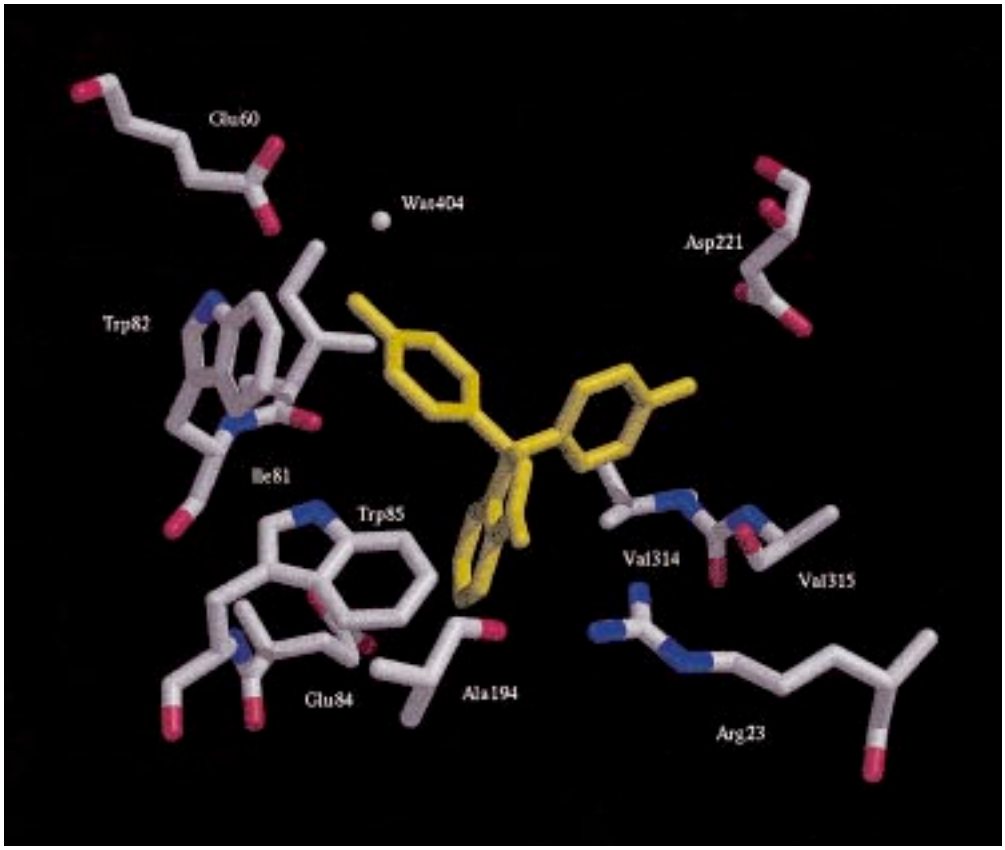


**Figure 2.** Detail of the X-ray crystal structure of the binary complex between LcTS and phenolphthalein.

**Scheme 1**[a]

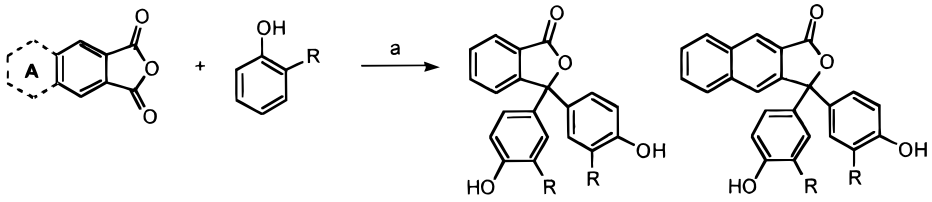


**1a,b** **2a-c**

| 1 | R | 2 | R |
|---|---|---|---|
| **a** | H | **a** | H |
| **b** | Cl | **b** | F |
| | | **c** | Cl |

[a] A = H, phenyl. (a) $H_2SO_4$, 180 °C, 5 h.

unsymmetrically substituted **1c** was obtained from the commercially available 2-(4′hydroxybenzoyl)benzoic acid by treatment with thionyl chloride and, in succession, α-naphthol (Scheme 2). Attempts to apply the method described above to 1,8-naphthalic anhydride for the 2,3-isomer failed, resulting in starting material being recovered in high amounts in addition to traces of compound **3** or **4**, depending on the starting phenol (Scheme 3).

An alternative pathway was therefore devised by adapting the procedure of Hubacher.[28] As shown in Scheme 4, the 1,8-naphthalic anhydride was heated at 130−140 °C with the appropriate phenol and aluminum

**Scheme 2**[a]

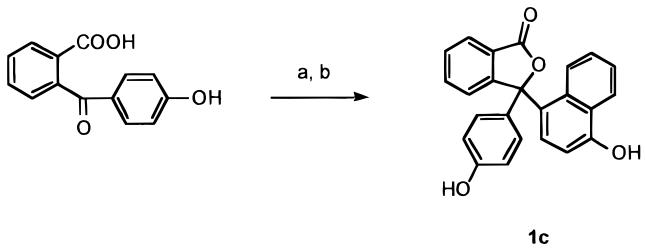


**1c**

[a] (a) $SO_2Cl$, 80 °C, 8 h; (b) α-naphthol.

chloride for 3 days. The still hot mixture was then poured onto ice and extracted with dichloromethane.

Scheme 3

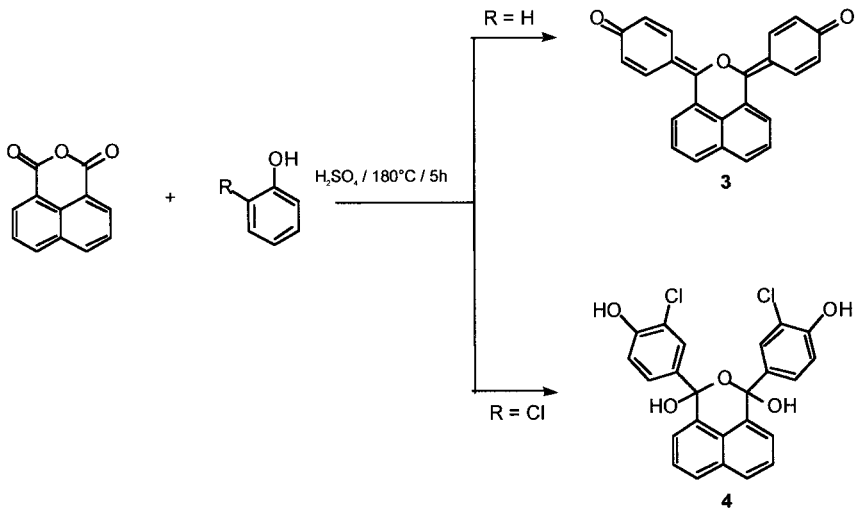


The insoluble residue was filtered off, the filtrate concentrated under vacuum, and the residue purified by silica gel chromatography to give, in elution order, the unreacted anhydride, compounds **5**, and the monosubstituted compounds **6**, whose presence was strongly dependent on the starting material. When phenol was used, together with the corresponding para-substituted **5a**, the *o*-phenol derivative **6a** was obtained. It should be noted that when using thymol the para-substituted compound **5** was not formed and only the ortho-monosubstituted **6d** was seen through $^1$H NMR (Scheme 4). The alkoxy derivatives **5d** and **6c** were synthesized by reacting **5a** and **6a**, respectively, with the appropriate alkyl halide in refluxing acetone and in the presence of potassium carbonate (Scheme 4, Table 1). Attempts to prepare **5d** starting from 1,8-naphthoic anhydride and anisole failed, since a concomitant demethylation took place, leading to **5a** as the sole reaction product. Following the same procedure described for compounds **5**, compound **7** was prepared starting from acenaphthene-5,6-dicarboxylic anhydride (Table 2 and Experimental Section).

Finally, it should also be noted that when starting from the 4-chloro- or 4-bromo-substituted 1,8-naphthalic anhydride, an approximately 60:40 mixture of the two possible isomers, **5aa** and **5ab**, **5ba** and **5bb** (Table 2), was obtained, as clearly indicated by $^1$H NMR spectra, while no monosubstituted products—as compounds **6**—were detected. Tables 3−5 report the biological activity of the above-mentioned compounds measured as isomeric mixtures. Future work involves the resolution of these isomers and testing their TS inhibition properties. In contrast, the presence of a 4-nitro group on the 1,8-naphthalic anhydride led to the formation of a single isomer for both **5** (**5ac**) and **6** (**6bc**) (Scheme 5 and Table 2).

## Results and Discussion

**Enzyme Inhibition.** All of the compounds were tested for their inhibitory properties against TS enzymes from different species: LcTS, PcTS, CnTS, and hTS. First, $K_i$'s were determined for each of the compounds against LcTS. Lineweaver−Burk (LB) analyses were performed for many of them in order to identify the mode of inhibition. Most of the compounds were shown to interfere with the folate cofactor activity and therefore behave as antifolates, as reported in Table 3. However, while most showed competitive inhibition with respect to the folate cofactor, two compounds (**6c**, **5ba**) displayed mixed-type inhibition. Compound **6bc** displayed noncompetitive inhibition. Analysis of the $K_i$'s of these compounds (Table 3) suggests that the semi-naphthalenic compound **6bc** is the best inhibitor of LcTS ($K_i$ of 0.25 $\mu$M), while compounds **5c**, **5aa**, and **5ba** show $K_i$'s of 0.7 $\mu$M. Many other compounds (**1b**, **2b**, **2c**, **5a**, **5b**, **5ab**, **5ac**, **7**) show $K_i$'s in the range of 1−2.8 $\mu$M. The least potent inhibitors are compounds **1c**, **5d**, and **6a**−**6d** ($K_i$ values ranging from 20.8 to higher than 290 $\mu$M). All of the compounds can be grouped into phthaleinic (**1a**−**1c**), 2,3-naphthalenic (**2a**−**2c**), 1,8-naphthalenic (**5a**−**5d**, **5aa**−**5bb**, **7**), and semi-naphthalenic structures (**6a**−**6d**, **6bc**). Among the phthaleinic compounds, the *o*-chloro substituent (compound **1b**) enhances the inhibitory activity of phenolphthalein (**1a**) 2.5-fold against LcTS, while compound **1c**, bearing an α-naphthol group, is about 4 times less active than PTH. This is likely due to the steric hindrance of the naphthol ring. In the 2,3-naphthalenic series, the *o*-halogen on the phenolic ring (compounds **2b**, **2c**) enhances the inhibitory potencies with respect to the unsubstituted compound (**2a**). As a group, the 1,8-naphthalenic compounds form the most interesting series: the semi-naphthalenic derivatives unsubstituted on the naphthalenic ring (**6a**−**6d**) showed low or very low inhibitory potencies (**6d**, $K_i$ = 26 $\mu$M; **6a**, $K_i$ = 104.7 $\mu$M; **6c**, $K_i$ = 295.6 $\mu$M), while the compound substituted at the naphthalenic ring is the most active compound among all those studied (**6bc**, $K_i$ = 0.25 $\mu$M). It should be noted that while compounds **6a**−**6c** have the phenolic hydroxyl in position 2, compound **6bc** has the phenolic hydroxyl in the 4-position, an *o*-chlorine group in the 3-position (ortho with respect to the phenolic hydroxyl), and a nitro group on the naphthalenic ring. The 1,8-naphthalenic derivatives (**5a**−**5d**), unsubstituted on the naphthalenic ring, show $K_i$ values ranging between 0.7 $\mu$M and 47% inhibition at 27 $\mu$M. The chlorine atom on the phenolic ring enhances the inhibitory activity: **5c** shows the lowest $K_i$ value (0.7 $\mu$M) in this series of

**Scheme 4**[a]

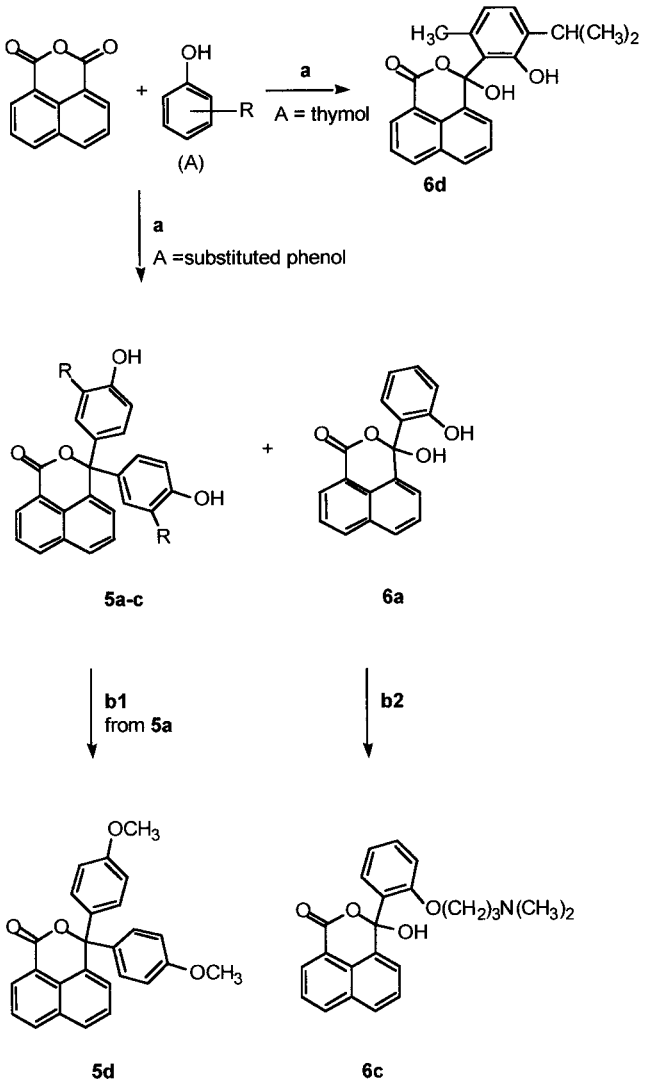


| 5 | R |
|---|---|
| a | H |
| b | F |
| c | Cl |

[a] (a) $AlCl_3$, 140 °C, 72 h; (b1) $CH_3I$, $K_2CO_3$, acetone; (b2) $(CH_3)NCH_2CH_2I$, $K_2CO_3$, acetone.

**Scheme 5**[a]

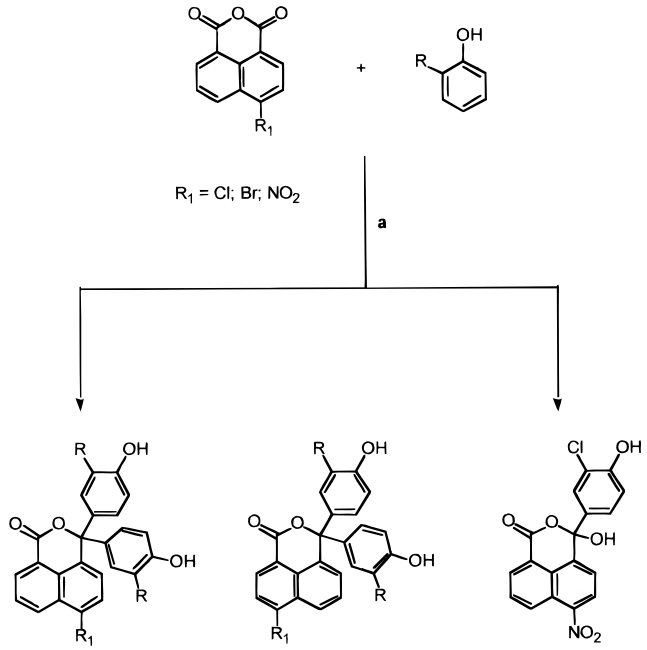


| 5, 5* | R | $R_1$ |
|---|---|---|
| aa | H | Cl |
| ab | H | Br |
| ac | H | $NO_2$ |
| ba | Cl | Cl |
| bb | Cl | Br |

[a] (a) $AlCl_3$, Δ (130/140 °C), 72 h.

compounds. That compound **5d** is much less active than **5a** (47% inhibition at 27 μM for **5d**, 2.8 μM for **5a**) implies that the substitution of the phenolic hydroxyl with a methoxy group blocks a key hydrogen bond interaction within the active site. 1,8-Naphthalenic derivatives such as chloro (**5aa**, **5ba**), bromo (**5ab**, **5bb**), or nitro (**5ac**) show promising inhibition, with $K_i$ values ranging between 0.7 and 1.7 μM. The exception to this trend is compound **5bb**, which has a slightly higher $K_i$ of 6.3 μM.

Since many of these compounds have one or two electron-withdrawing groups (halogen or nitro group) on the phenolic and/or naphthalenic rings but no large difference in inhibitory potency, it would seem that these functional modifications alone are not critical for the activity toward the LcTS enzyme. In particular, no improvement in the binding energy was observed in the 6/7-substituted 3,3-bis(4-hydroxyphenyl)-1*H*,3*H*-naphtho[1,8-*cd*]pyran-1-one derivatives implying that the substituents do not give specific interactions with any active site residue. It should be noted that the isomeric mixtures of 6/7-substituted compounds (**5aa** and **5ab**, **5ba** and **5bb**) were tested without separating the two isomers. Work in progress involves the separation of the isomeric mixtures and the testing of the two isomers. Finally, compound **7** shows a $K_i$ value of 1.5 μM. This is in the same range as compounds **5aa**, **5ab**, **5ac**, and **5ba**, which is in keeping with the above-described lack of specific interactions for this region of the compounds with active site residues.

Before conducting cell culture assays, inhibition factors (IF) were determined at a single inhibitor concentration (27 μM) against each of the four enzymes (LcTS, PcTS, CnTS, and hTS)[29,30] (Table 4). This approach consisted of measuring the single concentration inhibited and uninhibited initial rates of the enzyme reaction to give the IF value (see Experimental Section). This rapid method is utilized for efficient compound screening/profiling and to direct more detailed kinetic and in vitro experiments.

To evaluate the reliability of IF as an inhibitor of the biological activity of the compounds during the screening phase and to gain a significant biological profile, we studied the relationships for each compound between the $K_i$ measured against LcTS (Table 3) and the IF

**Table 1.** Physicochemical Data of Compounds **1**, 2, 5, and **6**

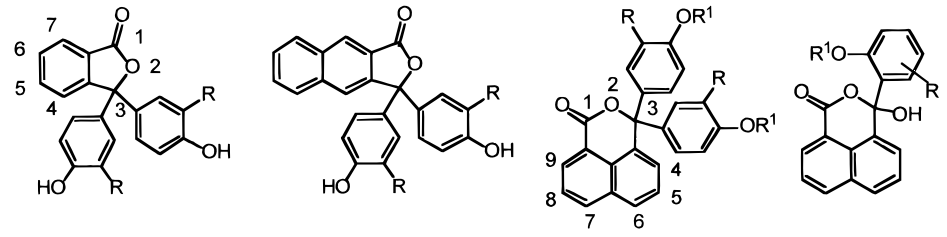

**1a,b** **2a-c** **5a-d** **6a,c,d**

| compd | R | $R^1$ | % yield | mp (°C) | formula[a] |
|---|---|---|---|---|---|
| **1b** | Cl | | 50 | 88−90 | $C_{20}H_{12}Cl_2O_4$ |
| **2a** | H | | 29 | 298−300 | $C_{24}H_{16}O_4$ |
| **2b** | F | | 30 | 135−140 | $C_{24}H_{14}F_2O_4$ |
| **2c** | Cl | | 35 | 200−205 | $C_{24}H_{14}Cl_2O_4$ |
| **5a** | H | H | 18 | 265−267 | $C_{24}H_{16}O_4$ |
| **5b** | F | H | 25 | 250−253 | $C_{24}H_{14}F_2O_4$ |
| **5c** | Cl | H | 9 | 162−165 | $C_{24}H_{14}Cl_2O_4$ |
| **5d** | H | $CH_3$ | 83[b] | 167−168 | $C_{26}H_{20}O_4$ |
| **6a**[c] | H | H | 15 | 175−178 | $C_{18}H_{12}O_4$ |
| **6c** | H | $(CH_2)_3$ | 40 | 160−163 | $C_{23}H_{23}NO_4$ |
| **6d**[c] | 3-$CH(CH_3)_2$ and 6-$CH_3$ | H | 12 | 192−193 | $C_{22}H_{20}O_4$ |

[a] Elemental analyses for the compounds were within ±0.4% of the theoretical values. [b] From **5a**. [c] $^1$H NMR spectra (DMSO-$d_6$) indicate the existence of a corresponding open form (see Supporting Information.

**Table 2.** Physicochemical Data of Compounds **5aa**−**bb**, **6bc**, and 7

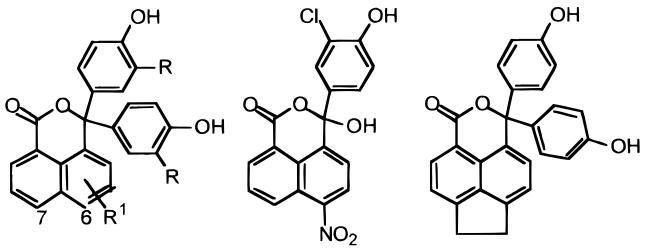

**5aa-bb** **6bc** **7**

| compd | R | $R_1$ | % yield | formula[a] |
|---|---|---|---|---|
| **5aa**[b] | H | 6(7)-Cl | 50 | $C_{24}H_{15}ClO_4$ |
| **5ab**[b] | H | 6(7)-Br | 12 | $C_{24}H^{15}BrO_4$ |
| **5ac** | H | 6-$NO_2$ | 10 | $C_{24}H_{15}NO_6$ |
| **5ba**[b] | Cl | 6(7)-Cl | 50 | $C_{24}H_{13}Cl_3O_4$ |
| **5bb**[b] | Cl | 6(7)-Br | 14 | $C_{24}H_{13}BrCl_2O_4$ |
| **6bc** | | | 10 | $C_{18}H_{10}ClNO_6$ |
| 7 | | | 10 | $C_{26}H_{18}O_4$ |

[a] Elemental analyses for the test compounds were within ±0.4% of the theoretical values. [b] As a 60/40 mixture of two isomers. See Supporting Information for $^1$H NMR data.

**Table 3.** Inhibition Constants ($\mu$M) against *L. casei* Thymidylate Synthase for Compounds **1**, 2, and 5−7

| compd[a] | $K_{iapp}$ | type of inhibition[b] |
|---|---|---|
| **1a**[c] (1) | 4.7 (33.1) | M/C |
| **1b** (6) | 1.9 | C |
| **1c** | 20.8 | C |
| **2a** (2) | 7.0 | C |
| **2b** | 1.5 | C |
| **2c** | 1.5 | C |
| **5a** (3) | 2.8 | C |
| **5b** | 1.6 | C |
| **5c** (4) | 0.7 | C |
| **5d** | 47% at 27 $\mu$M[d] | |
| **6a** | 104.7 | C |
| **6c** | 295.6 (764.0) | M |
| **6d** | 26 | C |
| **5aa**[e] | 0.7 | C |
| **5ab**[e] | 1.7 | C |
| **5ac** (5) | 1.0 | C |
| **5ba**[e] (7) | 0.73 (1.0) | M |
| **5bb**[e] | 6.3 | C |
| **6bc** (8) | 0.25 | NC |
| 7 | 1.5 | C |
| CB3717 | 0.095[f] | C |

[a] Number in parentheses refers to the corresponding compound in ref 27 for the convenience of the reader. [b] C, competitive inhibition; M, nonlinear mixed-type inhibition; NC, noncompetitive. Numbers in parentheses indicate $\alpha K_i$ for mixed-type inhibitor. [c] **1a** is phenolphthalein. [d] Percentage of inhibition at the indicated concentration. [e] 60/40 mixture of two isomers (see Table 2). [f] Reference 22.

against LcTS. The plot of log($K_i$) against log(IF) gives a linear relationship with a strong correlation factor ($R$ = 0.8122) between the two parameters (data not shown). This strong correlation between the two parameters prompted us to screen all the compounds using simple IF data as inidicators of the inhibitory properties. Inhibition factors for all the compounds against LcTS, PcTS, CnTS, and hTS are shown in Figure 3 where they are grouped by selectivity with respect to hTS. The selectivity is given by the ratio $IF_{hTS}/IF_{other\_species\_TS}$ (data not shown). In the top panel of Figure 3, the IF values against LcTS (blue) with respect to hTS (red) are reported and the compounds are ranked by increasing selectivity.

The majority of the compounds were ineffective toward hTS; only **1a**, **1c**, the phthalein derivatives, and 2c showed appreciable inhibitory activity with IF values between 0.103 and 0.182. The other derivatives were weakly active (**1b**, **2a**, **2b**, **5a**, **5aa**, **5ab**, **5ac**, 7) with IF values between 0.424 and 0.670 or inactive (**5b**, **5c**, **5d**, **6a**, **6c**, **6d**, **5ba**, **5bb**, **6bc**) ranging between 0.814 and 1. On the contrary, very interesting results were observed in the inhibition of LcTS. In particular, compounds **2c**, **5b**, **5c**, **5aa**, **5ab**, **5ba**, and **6bc** displayed IFs ranging from 0.070 to 0.129, while others (**1a**, **1b**, **2a**, **2b**, **5a**, **5ac**, **5bb**, 7) had inhibition factors < 0.5. Structure−selectivity analysis suggests that the 2,3-naphthalic anhydride derivative **2a** has the same in-

**Table 4.** Inhibition Factors (IF)[a] for Compounds **1**, **2**, and **5**−**7** against Thymidylate Synthease from Different Species

| compd | LcTS | PcTS | CnTS | hTS |
|---|---|---|---|---|
| **1a**[b] | 0.444 | 0.608 | 0.252 | 0.182 |
| **1b** | 0.470 | 0.725 | 0.704 | 0.670 |
| **1c** | 0.529 | 0.498 | 0.389 | 0.172 |
| **2a** | 0.247 | 0.459 | 0.215 | 0.594 |
| **2b** | 0.298 | 0.582 | 0.507 | 0.521 |
| **2c** | 0.093 | | | 0.103 |
| **5a** | 0.309 | 0.179 | 0.283 | 0.272 |
| **5b** | 0.096 | | | 1 |
| **5c** | 0.070 | 0.240 | 0.788 | 0.814 |
| **5d** | 0.624 | 0.749 | 0.836 | 1 |
| **6a** | 0.781 | 0.151 | 0.576 | 0.957 |
| **6c** | 0.768 | 0.928 | 0.666 | 1 |
| **6d** | 0.966 | 0.788 | 0.868 | 1 |
| **5aa**[c] | 0.092 | 0.632 | 0.256 | 0.438 |
| **5ab**[c] | 0.112 | 0.536 | 0.243 | 0.453 |
| **5ac** | 0.250 | 0.645 | 0.365 | 0.424 |
| **5ba**[c] | 0.129 | 0.488 | 0.120 | 1 |
| **5bb**[c] | 0.360 | | | 1 |
| **6bc** | 0.086 | 0.418 | <0.04 | 1 |
| **7** | 0.409 | 0.344 | 0.344 | 0.475 |
| CB3717 | <0.04 | <0.04 | <0.04 | <0.04 |

[a] IF = $V_{ii}/V_i$, ratio between the initial rate of the enzymatic reaction in the presence ($V_{ii}$) and absence ($V_i$) of the inhibitor at 27 $\mu$M. LcTS, *L. casei* TS; PcTS, *P. carinii* TS; CnTS, *Cr. neoformans* TS; hTS, human TS. [b] **1a** is phenolphthalein. [c] 60/40 mixture of two isomers (see Table 2).

hibitory activity against hTS (IF = 0.59) and microbial TS (IF = 0.21−0.45). Similar behavior is observed with the addition of a fluorine atom to the 3-position on phenolic rings (**2b**), while a chlorine atom at the 3-position (**2c**) gave increased activity against hTS while leaving the bacterial TS inhibition almost unchanged. Among the 1,8-naphthalic anhydride derivatives, the methylation of the phenolic hydroxyl gave an inactive compound (**5d**) against both LcTS and hTS, while the addition of an *o*-chlorine atom on the phenolic rings led to the derivative **5c**, which is 4-fold more potent and more selective against LcTS than the corresponding unsubstituted **5a**. Similar results were obtained when a chlorine (**5aa**) or bromine (**5ab**) atom was added to the naphthalenic ring. However, **5ba** and **5bb** are equipotent against LcTS; this suggests that these effects are neither additive nor synergistic.

Compounds **6bc**, **5c**, and **5ba**, characterized by the presence of an *o*-chlorine on the phenolic rings, are the most selective against LcTS versus hTS (Figure 3). It seems that the *o*-halogen substitution with chlorine is an important prerequisite for bacterial selectivity; the *o*-fluoro derivative of **5a** showed similar selectivity in the only molecule synthesized (**5b**).

The selective activities of these compounds against the TS from *P. carinii* are reported in the middle panel of Figure 3 with respect to hTS and are ranked by increasing selectivity. Only **5a**, **5c**, and **6a** showed interesting properties toward PcTS with IFs of 0.179, 0.240, and 0.151, respectively, while the others were devoid of significant activity. Compounds **1c**, **2a**, **5ba**, **6bc**, and **7** show IF values ranging between 0.344 and 0.498; compounds **1a**, **1b**, **2b**, **5d**, **6d**, **5aa**, **5ab**, and **5ac** show low inhibitory activity with IF values ranging between 0.536 and 0.788, while **6c** is almost inactive (Table 4 and Figure 3). The majority of the compounds (**1a**, **1c**, **5ac**, **5aa**, **5ab**, **2b**, **1b**) are less active against PcTS with respect to hTS. However, compounds **6c**, **6d**, **2a**, **5d**, **7**, and **5a** are slightly better inhibitors of PcTS than hTS, while compounds **5ba**, **6bc**, **5c**, and **6a** show some selectivity and significantly inhibit PcTS while remaining almost inactive against hTS (Figure 3). Also, in this regard, compounds **5c**, **5ba**, and **6bc** are among the most selective compounds: the ortho-position chlorine on the phenolic ring and the nitro group on the naphthalenic ring in both the 1,8-naphthalenic and 1,8-semi-naphthalenic derivatives confer selectivity to the compounds toward bacterial/pathogenic TSs with respect to the human enzyme.

In the bottom panel of Figure 3, IF values for CnTS versus hTS are reported and the compounds are ranked by increasing selectivity. Compounds **6bc** and **5ab** show IF values < 0.04 and 0.120, respectively. Compounds **1a**, **1c**, **2a**, **5a**, **5aa**, **5ab**, **5ac**, and **7** range from 0.215

**Table 5.** In Vitro Activity ($\mu$M) of Compounds **1**, **2**, and **5**−**7**

| | | MIC/MGC[b] | | | |
|---|---|---|---|---|---|
| compd | $CC_{50}$[a] MT-4 | *S. aureus* | *Streptococcus* | *Cr. neoformans* | SI[c] $CC_{50}/MIC_{Str.}$ |
| **1a**[d] | 58 | >58 | 38/58 | >58 | 1.5 |
| **1b** | 77 | 32/64 | 32/32 | >77 | 2.4 |
| **1c** | 54 | 17/54 | 8/34 | >54 | 6.7 |
| **2a** | 79 | 17/68 | 34/34 | >79 | 2.3 |
| **2b** | 94 | 15/30 | 15/15 | >94 | 6.2 |
| **2c** | 120 | 3.1/6.2 | 3.1/6.2 | >200 | 39.6 |
| **5a** | 41 | 34/41 | 17/34 | >41 | 2.4 |
| **5b** | 117 | 25/50 | 25/25 | >200 | 4.6 |
| **5c** | 46 | 7.0/14 | 1.8/3.5 | 9.37 | 25.5 |
| **5d** | 21 | >21 | >21 | >21 | |
| **6a** | 263 | >263 | 171/263 | 18.7 | 1.5 |
| **6c** | 70 | >70 | >70 | >70 | |
| **6d** | 89 | >89 | 72/>89 | >89 | 1.2 |
| **5aa**[e] | 69 | 8/16 | 8/8 | >69 | 8.6 |
| **5ab**[e] | 76 | 7.0/28 | 7.0/28 | 37.5 | 10.8 |
| **5ac** | 41 | 15/30 | >41 | >41 | |
| **5ba**[e] | 63 | 3/3 | 1.6/1.6 | 9.37 | 39.4 |
| **5bb**[e] | 154 | 3.1/12.5 | 3.1/3.1 | >200 | 49.6 |
| **6bc** | 66 | 4/17 | 8/8 | >66 | 8.25 |
| **7** | 53 | 16/32 | 16/32 | >53 | 3.3 |

[a] $CC_{50}$, compound dose necessary to reduce the viability of mock-infected cells at 50%. [b] MIC/MGC, minimum compound dose able to inhibit bacterial growth/lowest compound dose with germicidal effect. [c] SI, selectivity index given by $CC_{50}/MIC_{Streptococcus}$ ($CC_{50}/MIC_{Str.}$). [d] **1a** is phenolphthalein. [e] 60/40 mixture of two isomers (see Table 2).

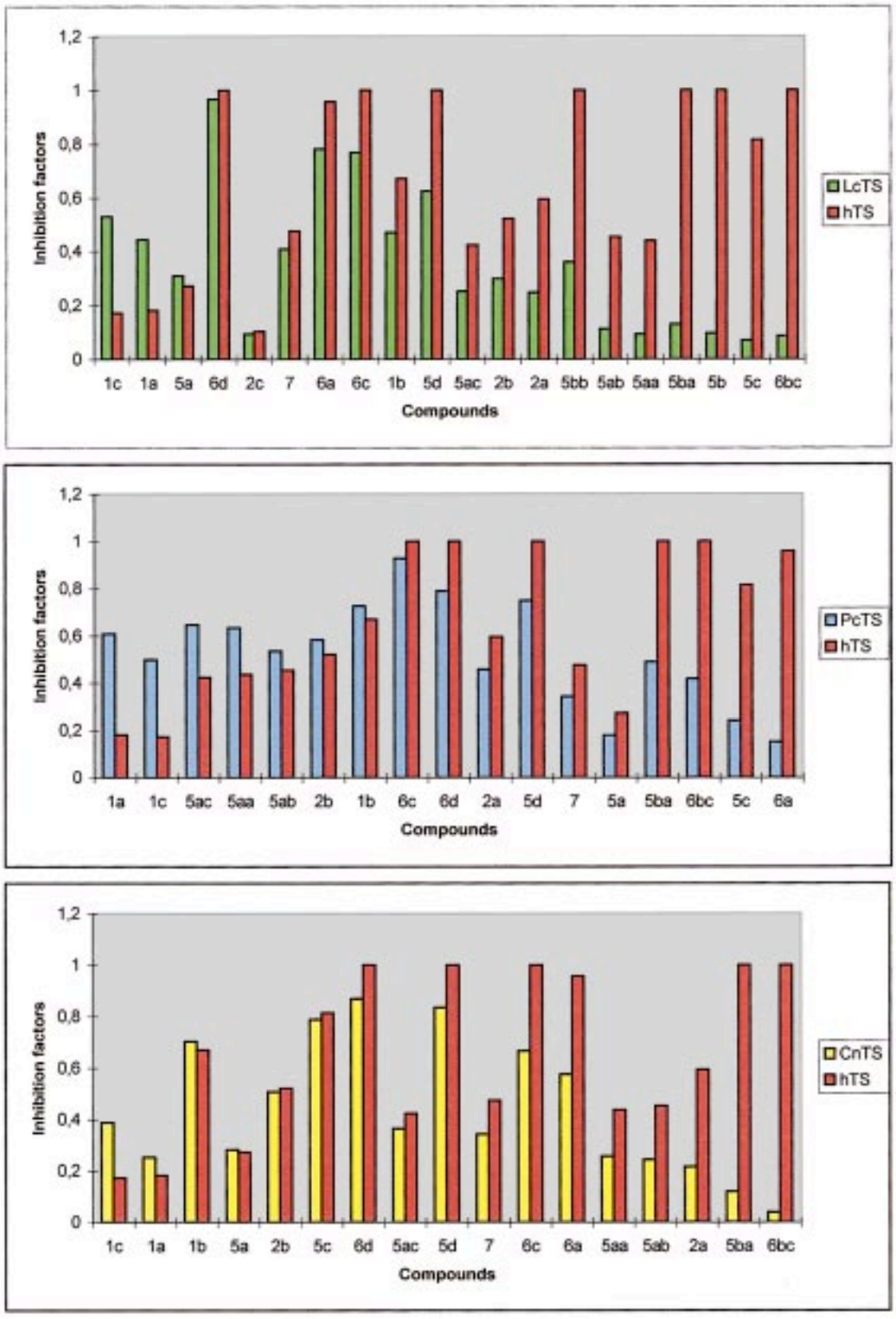


**Figure 3.** Plot of the inhibition factors (IF) at 27 $\mu$M of compounds **1**, 2, and 5−7 toward TS from *L. casei. P. carinii, Cr. neoformans*, and human. IFs are grouped by selectivity with respect to human TS, and the compounds are ranked by increasing selectivity.

to 0.389, while **1b**, **2b**, **6a**, and **6c** show IFs ranging between 0.507 and 0.704. Finally, **5c**, **5d**, and **6d** display IF values higher than 0.789. In general, the compounds are more active against CnTS than PcTS (Table 4). With regard to selectivity, compounds **1c**, **1a**, **1b**, **5a**, **2b**, and **5c** display essentially the same inhibition potency toward both PcTS and hTS (Figure 3). Compounds **6d**, **5ac**, **5d**, and **7** are slightly less potent against hTS with respect to CnTS, while **6c**, **6a**, **5aa**, **5ab**, and **2a** show higher selectivity. Finally, compound **6bc** showed an IF

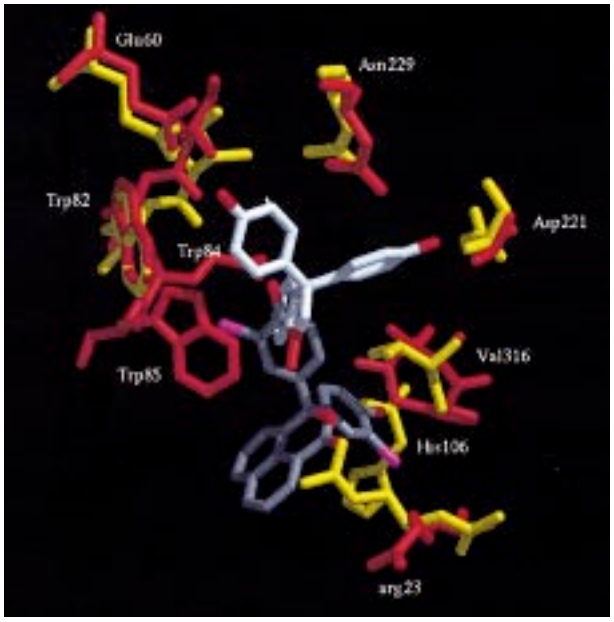


**Figure 4.** Superimposition of the X-ray crystal structures of the binary complexes of LcTS−PTH (in white, yellow residues) and LcTS−5c (in gray, red residues).

< 0.04 against CnTS, while being inactive in the hTS assay, thus displaying a potentially high selectivity with respect to these two enzymes. To a lesser extent, compound **5ba** also showed some selectivity with respect to CnTS.

The most potent and selective compound against CnTS is the nitro derivative **6bc** whose structure is "semi-naphthalenic" with the substitution of a hydroxyl group for one of the phenolic rings. Since compounds **6a**, **6c**, **6d**, and **7** showed no particular selectivity or potency, it is apparent that both the hydroxyl substitution for the phenol ring and the nitro group are crucial to the activity and selectivity of this molecule. Finally, compounds **3** and **4**, whose structures are symmetric, were devoid of activity.

The biological activity profile of the classic antifolate inhibitor CB3717 was compared to that of the present compounds: $K_i$ values against LcTS, PcTS, CnTS, and hTS were all very similar (0.095,[22] 0.09,[22] 0.075, 0.18 $\mu$M[22]), indicating that no selectivity is observed for this classical TS inhibitor. As a very potent inhibitor of TS, the IF values for CB3717 are lower than 0.04.

The molecular recognition of these unusual antifolates, examined through the analyses of the X-ray crystal structures of the binary complexes of compound **5c** with LcTS and of compound **5ac** with LcTS,[27] showed that these naphthalene derivatives occupy different binding sites than has been observed for compounds **1a**[26] (PTH) and CB3717.[9] Figure 4 shows details of the crystal structure of the LcTS−**5c** binary complex (**5c** in gray, residues in red) superimposed on the LcTS:PTH binary complex (PTH in white, residues in yellow). It can be noted that a different conformation must be adopted by the enzyme to accommodate compound **5c** in this binding site, where it forms close interactions with Arg23, His106, and Val316. These interactions are discussed in detail elsewhere.[27]

**In Vitro Assays.** Following the initial enzymatic screen, the cytotoxicity of phenolphthalein (**1a**) and its derivatives were evaluated in vitro in two CD4+ lymphocyte cell lines: MT-4 and C8166. Compounds were also evaluated for antiviral activity against two different RNA viruses, human immunodeficiency virus (HIV) and human rhinovirus (HRV), as well as against two DNA viruses, such as vaccinia (VV) and herpes simplex (HSV). The antibacterial activity was tested against Gram-positive (*Staphylococcus aureus*, group D *Streptococcus*), Gram-negative (*Pseudomonas aeruginosa*, *Salmonella sp.*), and acid-fast (*Mycobacterium avium*, *M. tuberculosis*), "microorganisms", whereas the antimycotic activity was evaluated against *Candida albicans*, *C. parapsilosis, C. paratropicalis,* and *Cryptococcus neoformans*. All of the studied compounds, with the exception of the more active **5d** and of the less active **2c**, **5b**, **5bb**, and **6a**, showed a similar low degree of cytotoxicity for MT-4 cells (Table 5), with $CC_{50}$ values ranging from 41 to 94 $\mu$M. Compound **5d** showed a $CC_{50}$ value of 21 $\mu$M, and compounds **2c**, **5b**, **5bb**, and **6a** were only slightly cytotoxic or not cytotoxic at all. Similar results were obtained with C8166 cells (data not shown). When evaluated for their ability to prevent virus-induced cytopathogenicity in cell cultures infected at low multiplicities of infection, none of the compounds were found to inhibit the multiplication of HIV-1 (data not shown). On the other hand, **1a** was active against two HRV strains, HRV-2 and HRV-14, at concentrations (45 $\mu$M) that, although close to the $CC_{50}$ value for MT-4, were not cytotoxic for HeLa cells, suggesting a selective inhibition of rhinoviruses (data not shown). Plaque reduction assays revealed that the compounds were inactive against both vaccinia and HSV (data not shown). With respect to antibacterial activity, all of the compounds were inactive against *P. aeruginosa* and *Salmonella sp.*, whereas some of them inhibited the growth of both *Staphylococcus* and *Streptococcus* (Table 5). Compounds **5ba**, **5c**, **5bb**, **2c** > **5aa**, **6bc**, **5ab** were, in the order of decreasing potency, the most active compounds. These compounds showed minimum inhibitory concentrations (MIC) ranging between 1.6 and 8 $\mu$M and minimum germicidal concentrations (MGC) ranging between 1.6 and 28 $\mu$M. These concentrations were well below those found to be cytotoxic for T-cell lines. This suggested a selective mode of inhibition. When evaluated for antimycotic activity, none of the compounds inhibited the multiplication of the various *Candida* strains. However, several phenolphthalein derivatives were selective inhibitors of *Cr. neoformans*, the most potent compounds being **5c**, **5ba**, **5ab**, and **6a** active at doses ranging between 9.4 and 37.5 $\mu$M.

The qualitative structure−activity relationship in *Staphylococcus* and *Streptococcus* cell culture shows that the introduction of a chlorine atom on the phenolic ring of 1,8-naphthalene derivatives (cf. **5a** with **5c**, **5aa** with **5ba**, **5ab** with **5bb**) increases either the activity (i.e., 17/34 $\mu$M (**5a**) 1.8/3.5 $\mu$M (**5c**)) or the selectivity (i.e., 2.4 $\mu$M (**5a**) 25.5 $\mu$M (**5c**)). The same behavior is found with 2,3-naphthalene derivatives. Compound **2c** is more active and selective than **2a**. The substitution of the phenolic OH with a $-OCH_3$ group (cf. **5a**, **5d**, **6a**, **6d**) and of the phenol ring with an OH group (cf. **5a**, **6a**) reduces the activity.

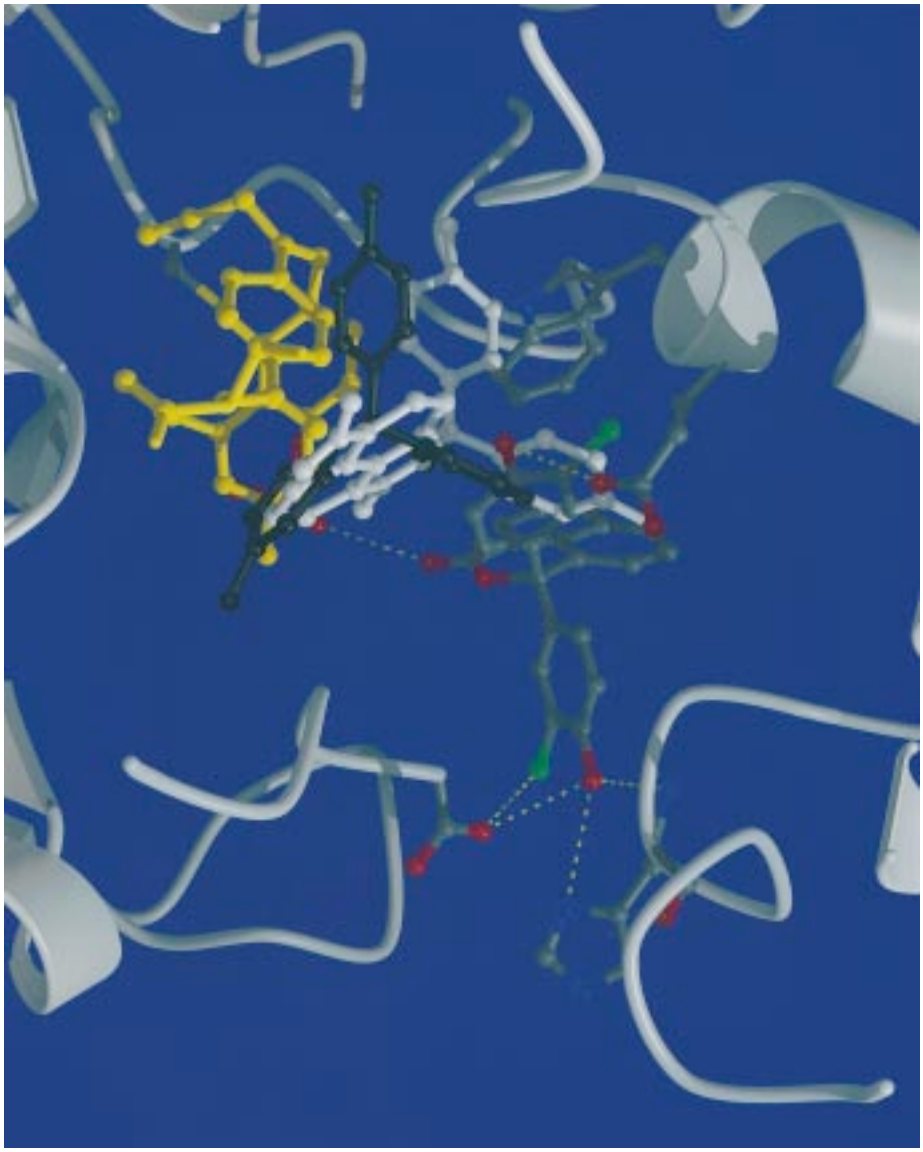

**Figure 5.** Superimposition of the X-ray complexes of PTH (black), CB3717 (yellow), **5ac** (white), and **5c** (gray).

## Conclusions

With the LcTS:PTH crystal structure as a starting point, we have been able to design a new class of naphthalenic TS inhibitors which specifically target interactions within the enzyme's active site which are unique to bacterial and mycotic species. As a result, several rounds of structure-guided inhibitor design have led to compounds with both enhanced potency of a high degree of species specificity. The best compounds in this series show nanomolar inhibition of bacterial TSs, while leaving hTS unimpeded even at the solubility limits of the compounds (200 $\mu$M). Structure−activity analysis of these compounds against LcTS showed that many functional variations can be made on the naphthalenic core without significantly altering the compounds' binding affinities, from which we conclude that this portion of the chemical scaffold is not crucial to inhibitory activity. In contrast, small modifications on the phenol ring moieties, such as the introduction of chlorine at the ortho-position, significantly alter the selectivity alter the selectivity alter the selectivity properties of the molecules. Crystal structures of two binary complexes of LcTS with compounds in this series (**5c**, **5ac**) both validated the specificity effects shown by modifications of the phenol moieties and explained the promiscuity of derivitizations on the naphthalenic core.[27] These structures showed that the C6−C7 edge of the naphthalenic ring system is directed toward a large cavity within the active site where there are no close contacts made with the protein, while the phenol rings make distinct, tight interactions with residues from an amino acid insertion unique to bacterial and mycotic forms of the enzyme.

Since this new class of TS inhibitors was designed to be selective against human TS, these compounds were evaluated for their antibacterial activity as well as for efficacy against opportunistic pathogens whose infections are often lethal in disorders arising from HIV and cancer therapies. All of the compounds were initially screened for biological activity using the relatively simple inhibition factor (IF) assay. The results of this first-pass analysis were used to direct more detailed kinetic experiments, greatly accelerating the design, synthesis, and evaluation stages while also minimizing the expenditure of material and resources. Enzymatic assays show that this class of compounds is unusually

selective for bacterial and mycotic TS versus human TS, being able to inhibit LcTS and CnTS at much lower concentrations than required for hTS. To our knowledge, no selective TS inhibitors have been reported to date with the exception of some patented compounds.[21] The in vitro assays are, in general, in good agreement with the enzymatic results. The naphthalene derivatives are only slightly or not cytotoxic and show antibacterial activity against *S. aureus* and *Streptococcus*. Unexpectedly, compounds **5c** and **5ba** were also active against *Cr. neoformans*. The most divergent result involves compound **6bc**, which, though very active against CnTS in the enzyme assay, as reported above, did not retain this activity in the in vitro assay. This inconsistency may be due to poor membrane penetration or, possibly, metabolic transformations.

Unlike the classic antifolates, all of these compounds lack the pteridine-like moiety and the glutamate "tail" present in the common antifolate-based TS inhibitors. Since these compounds do not resemble folates chemically, in the biological setting they are also not constrained to interactions with the RFC−FPGS system thereby reducing the potential for the development of resistance mechanisms. Given the dramatic rise in antibiotic resistance and the problems of opportunistic infections among the immunocompromised, new chemical classes of antimicrobials, such as these compounds, are much needed.

## Experimental Section

**Chemistry.** Phenolphthalein (PTH), 1,8-naphthalic anhydride, 2,3-naphthalic anhydride, and 4-hydroxybenzoylbenzoic acid were purchased from Aldrich-Chemie. Melting points were determined on a Büchi 510 capillary melting points apparatus and are uncorrected. Elemental analyses for the test compounds were within ±0.4% of the theoretical values. $^1$H NMR spectra were recorded on a Bruker MX400 WB spectrometer. DMSO-$d_6$ was used as the solvent, unless otherwise noted. UV spectra were determined using a Perkin Elmer UV spectrophotometer model lambda 16, equipped with a multicell system which was temperature regulated with a Haake F3C circulating bath. All of the compounds were characterized through mono- and bidimensional $^1$H NMR, and the data are enclosed as Supporting Information. TLC on silica gel plates was used to check product purity. Silica gel 60 (Merck; 70−230 mesh) was used for column chromatography. Flash chromatography was performed using silica gel 60, 200−400 mesh (Merck art. 9385). The structures of all compounds were consistent with their analytical and spectroscopic data. The stock solutions of the inhibitors were prepared in 100% DMSO and stored at −20 °C until use. The stability of the stock solutions of the compounds was monitored with time by spectrophotometric UV analysis; the spectra all remained unchanged throughout the course of these experiments. The solvent systems used in the enzymatic assays include DMSO and TES buffer (*N*-tris(hydroxymethyl)methyl-2-aminoethanesulfonic acid) (50 mM) at pH 7.4, $MgCl_2$ (25 mM), formaldehyde (6.5 mM), EDTA (ethylenediaminetetraacetic acid) (1 mM), and 2-mercaptoethanol (75 mM).

**3,3-Bis(4-hydroxyphenyl)-1(3*H*)-isobenzofuranone Derivatives (1), 3,3-Bis(4-hydroxyphenyl)-3*H*-naphtho[2,3-*c*]furan-1-one Derivatives (2), 1,3-Bis(*p*-quinonyl)-1*H*,3*H*-benzo[*de*]isochromon (3), and 1,3-Bis(3-chloro-4-hydroxyphenyl)-1,3-dihydroxy-1*H*,3*H*-benzo[*de*]isochromon (4): General Method.** A mixture formed by the required naphthalic or 2,3-naphthalic anhydride (0.01 mol), the appropriate phenol (0.02 mol), and several drops of $H_2SO_4$ was heated while stirring at 180 °C for 5 h. After cooling, the residue was purified by silica gel chromatography eluting with dichloromethane/methanol (95/5 v/v) to give the unreacted anhydride followed by the desired 1 or 2 (analytical data, Table 1; $^1$H NMR data, Supporting Information).

Compounds **3** and **4**, respectively, were obtained using the same method, by condensing 1,8-naphthoic anhydride with phenol or *o*-chlorophenol (Scheme 3). For **3**: yield 10%; $^1$H NMR (DMSO-$d_6$) $\delta$ 6.95 (d, 4H), 7.80 (d, 4H), 8.00 (t, 2H), 8.60 (d, 4H). For **4**: yield 8%; $^1$H NMR (DMSO-$d_6$) $\delta$ 7.01 (t, 2H), 7.11 (d, 2H), 7.28 (dd, 2H), 7.37 (dd, 2H), 7.42 (dd, 2H), 7.57 (d, 2H), 9.29 (s, 2H, exch with $D_2O$), 10.37 (s, 2H, exch with $D_2O$).

**3,3-Bis(4-hydroxyphenyl)-1*H*,3*H*-naphtho[1,8-*cd*]pyran-1-one Derivatives (5a, 5b, 5c), 3-Hydroxy-3-(hydroxyphenyl)-1*H*,3*H*-naphtho[1,8-*cd*]pyran-1-one Derivatives (6a, 6c), and Their Analogues Substituted at the Naphthalene Ring [5(5*)aa,ab,ac,ba,bb; 6bc]: General Method.** To a mixture of 1,8-naphthalic anhydride (0.01 mol) and the appropriately substituted phenol (0.02 mol) in 1,1,2,2-tetrachloroethane (100 mL) was added aluminum chloride (0.02 mol) portionwise at room temperature, and the suspension was stirred for 3 days at 110−115 °C. The still-hot mixture was then poured onto ice to which was added 200 mL of dichloromethane. After stirring for 0.5 h, the precipitate was filtered off and the organic layer separated and dried over sodium sulfate. After evaporation of the solvent, the residue was purified by silica gel chromatography, eluting with dichloromethane/methanol (95/5 v/v). The unreacted anhydride eluted first, followed by the bis- (5) and mono- (6) substituted phthaleins. Compounds substituted at the naphthalenic ring were obtained from the required 1,8-naphthalic anhydride and the appropriate phenol, following the same procedure. It should be noted that in this case a mixture of 6- or 7-substituted compounds (5, 5*) was obtained, as clearly evidenced by their $^1$H NMR spectra. Though attempts are in progress to separate the isomers, in this study they were evaluated as such.

Finally, compound **6d** was obtained according to the same method, starting from 1,8-naphthalic anhydride and thymol (analytical data, Tables 1 and 2; $^1$H NMR data, Supporting Information).

**7,7-Bis(4-hydroxyphenyl)-5*H*,7*H*-1,3-dihydro-6-oxacyclopenta[*cd*]phenalen-5-one (7).** Following the method described above, compound **7** was obtained starting from 1,2-dihydro-6-oxacyclopenta[*cd*]phenalene-5,7-dione (acenaphthene-5,6-didecarboxyanhydride): mp 232−235 °C (analytical data, Table 2; $^1$H NMR data, Supporting Information).

**3,3-Bis(4-methoxyphenyl)-1*H*,3*H*-naphtho[1,8-*cd*]pyran-1-one Derivatives (5d) and 3-Hydroxy-3-[(3-dimethylaminoprop-2-yl)oxy]-1*H*,3*H*-naphtho[1,8-*cd*]pyran-1-one (6c).** A mixture of the required **5a** or **6a** (1.35 mmol), the appropriate alkyl halide (2.7 mmol), and potassium carbonate (2.7 mmol) in acetone (5 mL) was refluxed for 4 h. The solvent was evaporated and the residue treated with water (3 mL) and extracted with diethyl ether (3 × 5 mL). After evaporation of the solvent, the residue was purified by silica gel chromatography eluting with dichloromethane/methanol (98/2 v/v), followed by crystallization from chloroform (Table 1 for data).

**3-(4-Hydroxyphenyl)-3-(4-hydroxynaphthyl)-1(3*H*)-isobenzofuranone (1c).** A mixture of 2-(4-hydroxybenzoyl)-benzoic acid (8.2 mmol) and thionyl chloride (5 mL) was refluxed for 8 h. After cooling, the excess thionyl chloride was evaporated under vacuum and the residue dissolved in toluene (5 mL) and added dropwise to a solution of α-naphthol (8.2 mmol) in toluene (5 mL). After stirring for 2 h at 40 °C, the mixture was cooled and the precipitate filtered under vacuum and purified by silica gel chromatography, eluting with cyclohexane/ethyl acetate (70/30 v/v): yield 70%; mp 255−258 °C; $^1$H NMR (DMSO-$d_6$) $\delta$ 6.8 (dd, 3H), 7.0 (d, 2H), 7.2 (d, 1H), 7.3−7.4 (m, 2H), 7.5−7.6 (m, 2H), 7.8−8.0 (m, 3H), 8.2 (d, 1H), 9.6 (s, 1H, exch with $D_2O$), 10.6 (s, 1H, exch with $D_2O$).

**Biochemistry and Biology. 1. Enzymology. Purification of the enzyme**: Plasmids that express *L. casei* TS in the Thy *E. coli* strain $\chi$2913 have been previously described.[31] The enzyme was purified by column chromatography using phosphocellulose (P11, Biorad) and hydroxyapatite (HAP, Biorad) resin, using phosphate buffer as the eluent.[32] TS enzymes

purified from *Cr. neoformans*, *P. carinii*, and human were purified as reported.[33−35] The enzyme preparations were >95% homogeneous as visualized by SDS (sodium dodecyl sulfate)−polyacrylamide gel electrophoresis. The purified enzymes were stored at −80 °C in 10 mM phosphate buffer, pH 7.0, and 0.1 mM EDTA.

Enzyme activity was determined spectrophotometrically by steady-state kinetic analysis, following the increasing absorbance at 340 nm due to the oxidation reaction of $N^5$,$N^{10}$-methylenetetrahydrofolate to dihydrofolate.[36] 1 mL of reaction solution was formed by standard assay buffer pH 7.4, dUMP (120 $\mu$M), 6(*R*,*S*)-1-$CH_2CH_4$-folate (140 $\mu$M), enzyme (0.07 $\mu$M). Assays were performed at 20 °C in the standard assay buffer formed by TES (*N*-tris(hydroxymethyl)methyl-2-aminoethanesulfonic acid) (50 mM) at pH 7.4, $MgCl_2$ (25 mM), formaldehyde (6.5 mM), EDTA (1 mM), and 2-mercaptoethanol (75 mM).

**Assays**: Stock solutions of the inhibitors were prepared in DMSO (dimethyl sulfoxide) and stored at −20 °C until use. The inhibition pattern for all of the compounds has been determined by steady-state kinetic analysis of the dependence of folate concentration from TS enzyme activity at varying inhibitor concentrations. For the most part, the compounds showed competitive or nonlinear intersecting mixed-type inhibition. Therefore, $K_i$ values have been measured in the first case, and $K_i$ and $\alpha K_i$ values have been determined in the second case.[37] Only a few compounds showed noncompetitive inhibition. For those compounds that showed competitive inhibition, $K_i$ values were obtained from the linear least-squares fit of the residual activity as a function of inhibitor concentration to the suitable equations for competitive inhibition.[38] Each of the experiments were repeated at least three times, and no individual measurement differed more than 10% from the mean.

The inhibition factors were determined as follows: the experiments were performed on each compound at a single concentration of 27 $\mu$M. The screening assay was done on the enzymes from *L. casei*, *P. carinii*, *Cr. neoformans*, and human to evaluate the species specificity of the synthesized compound. The assay conditions were those of the standard TS assay. Assays were performed at 20 °C in the standard assay buffer described above. A new reaction mixture (1 mL) was formed using standard assay buffer at pH 7.4 and the substrate, dUMP, at 120 $\mu$M; however, the folate concentration used was 60 $\mu$M, because the $K_m$'s of folate for each of the enzymes are similar (15.7 $\mu$M for PcTS, 10 $\mu$M for LcTS, 20 $\mu$M for CnTS, 8 $\mu$M for hTS). TS assays were performed in the absence and presence of each inhibitor, the respective initial rates were considered, and the ratio between the initial rate in the presence ($V_{ii}$) and in the absence ($V_i$) of each inhibitor gave the respective inhibition factors (IF = $V_{ii}/V_i$). Each of the inhibition factors was determined a minimum of three times, and no individual measurement differed more than 10% from the mean.

The effect of increasing DMSO concentration in the TS assay mixture was studied, and it was observed that no change in TS activity is seen at concentrations up to 10% DMSO.[39]

**2. In Vitro Assays. Compounds**: Since the test compounds have poor aqueous solubility, they were dissolved in DMSO at an initial concentration of 300 mM and then serially diluted in culture medium.

**Cells**: Cell lines were from American Type Culture Collection (ATCC); bacterial and fungal strains were either clinical isolates (obtained from Clinica Dermosifilopatica, University of Cagliari) or collection strains from ATCC. H9/IIIB, MT-4, and C8166 cells (grown in RPMI 1640 containing 10% fetal calf serum (FCS), 100 U/mL penicillin G, and 100 $\mu$g/mL streptomycin) were used for anti-HIV assays. HeLa Ohio cells were used for anti-HRV assays, whereas Vero cells were used for anti-VV and anti-HSV assays. Cell cultures were checked periodically for the absence of mycoplasma contamination with a MycoTect kit (Gibco).

**Viruses**: Human immunodeficiency virus type-1 (HIV-1, IIIB strain) was obtained from supernatants of persistently infected H9/IIIB cells. The cytopatic effect (CPE) of HIV-1 consists in the formation of syncitia; therefore it is not possible to calculate the vial titer as plaque-forming units (PFU). For this reasons the titer of HIV stock solutions is referred to as cell culture infectious dose 50 ($CCID_{50}$). The titer of the HIV-1 stock solution used throughout this study had titer of $6 \times 10^6$ $CCID_{50}$/mL. Stock solutions of HRV types 2 and 14 had titers of 4 and $8 \times 10^6$ PFU/mL, respectively.

**Antiviral assays**: Activity of compounds against the HIV-1 and HRV-2/HRV-14 multiplication in acutely infected cells was based on inhibition of virus-induced cytopathogenicity in MT-4 and HeLa Ohio cells, respectively. Briefly, 50 $\mu$L of culture medium (RPMI 10% FCS in the case of HIV-1; D-MEM 2% FCS, 30 mM $MgCl_2$, 15 $\mu$g/mL DEAE-dextran in the case of HRVs) containing $1 \times 10^4$ cells was added to each well of flat-bottomed microtiter trays containing 50 $\mu$L of medium with or without various concentrations of test compounds; 20 $\mu$L of HIV-1, HRV-2, or HRV-14 suspensions containing 100 $CCID_{50}$ was then added. After a 4-day incubation at 37 °C (3 days at 33 °C for the HRV-infected cultures), the number of viable cells was determined by the 3-(4,5-dimethylthiazol-2-yl)-2,5-diphenyltetrazolium bromide (MTT) method.[40] The cytotoxicity of compounds was evaluated in parallel with their antiviral activity. It was based on the viability of mock-infected cells, as monitored by the MTT method. The activity of test compounds against VV and HSV was tested in classical plaque reduction assays.[41]

**Antibacterial assays**: *S. aureus*, group D *Streptococcus*, *P. aeruginosa*, and *Salmonella sp.* were recent clinical isolates. Tests were carried out in nutrient broth, pH 7.2, with an inoculum of $10^3$ cells/tube. MICs were determined after 18 h of incubation at 37 °C in the presence of serial dilutions of the test compounds.

**Antimycotic assays**: Yeast blastospores were obtained from a 30-h-old shaken culture incubated at 30 °C in Sabouraud dextrose broth. The dermatophyte inoculum was scraped aseptically with a spatula from a 7-day-old culture on agar, and the macerate was finely suspended in Sabouraud dextrose broth using a glass homogenizer. Glycerol, final concentration 10%, was added as a cryoprotective agent to both yeast and dermatophyte suspensions, aliquots of which were then stored in liquid nitrogen. Test tubes were inoculated with $10^3$ blastospores or colony-forming units (CFU)/tube. The minimal inhibitory concentration (MIC) was determined by serial dilutions using Sabouraud dextrose broth (pH 5.7) and incubating at 37 °C. The growth control for yeasts was read after 1 day and for dermatophytes after 3 days (5 days for *Cr. neoformans*). The MIC was defined as the compound concentration at which no macroscopic signs of fungal growth were detected. The minimal germicidal concentration (MGC) was evaluated by subcultivating negative test tubes in Sabouraud dextrose agar, without the inhibitors, and represents the lowest dose of compound with germicidal effect.

**Acknowledgment.** This work was supported by Consiglio Nazionale delle Richerche (CNR) (P.P.) and Ministero della Ricerca Scientifica e Tecnologica Italiano (MURST) (M.P.C.) (60%). Thanks are due to Centro Interdipartimentale Grandi Strumenti Università di Modena (CIGS) and Centro Interdipartimentale di Calcolo Elettronico (CICAIA) for computing facilities, to Dr. Brian Shoichet and Prof. I. D. Kuntz for critical reading of the manuscript, to Rossella Gallesi of the Microanalyses Laboratory, and to Fabrizia Soragni of Dipartimento di Scienze Farmaceutiche Università di Modena for her excellent technical assistance.

**Supporting Information Available**: NMR characterization of the compounds. This material is available free of charge via the Internet at http://pubs.acs.org.

## References

(1) Douglas, K. T. The Thymidylate Synthesis Cycle and Anticancer Drugs. *Med. Res. Rev.* **1987**, *7*, 441−475.

(2) Harrison, P. T.; Scott, J. E.; Hutchinson, M. J.; Thompson, R. Site-directed mutagenesis of Varicella-zoster virus Thymidylate Synthase. Analysis of two highly conserved regions of the enzyme. *Eur. J. Biochem.* **1995**, *230*, 511−516.
(3) Schultz, R. M. Newer antifolates in Cancer Therapy. *Prog. Drug. Res.* **1995**, *44*, 129−157.
(4) Santi, D. V.; Danenberg, P. V. In *Folates and Pterins: Vol. 1, Folate in Pyrimidine Nucleotide Biosynthesis*; Blakley, R. L., Benkovic, S. J., Eds.; John Wiley & Sons: New York, 1984; pp 345−399.
(5) Carreras, C. W.; Santi, D. V. The catalytic mechanism and structure of thymidylate synthase. *Annu. Rev. Biochem.* **1995**, *64*, 721−762.
(6) Hardy, L. W.; Finer-Moore, J. S.; Montfort, W. R.; Jones, M. O.; Santi, D. V.; Stroud, R. M. Atomic structure of thymidylate synthase: target for rational drug design. *Science* **1987**, *235*, 448−455.
(7) Knighton, D. R.; Kan, C. C.; Howland, E.; Janson, C. A.; Hostomska, Z.; Welsh, K. M.; Matthews, D. A. Structure of and kinetic channelling in bifunctional dihydrofolate reductase-thymidylate synthase. *Nature Struct. Biol.* **1994**, *1*, 186−194.
(8) Kamb, A.; Finer-Moore, J. S.; Calvert, A. H.; Stroud, R. M. Structural basis for recognition of polyglutamyl folates by thymidylate synthase. *Biochemistry* **1992**, *31*, 9883−9890.
(9) Matthews, D. A.; Appelt, K.; Oatley, S. J.; Xuong, N. H. Crystal structure of Escherichia coli thymidylate synthase containing bound 5-fluoro-2′-deoxyuridylate and 10-propargyl-5,8-dideazafolate. *J. Mol. Biol.* **1990**, *214*, 923−936.
(10) Stroud, R. M. Unpublished.
(11) Matthews, D. A.; Villafranca, J. E.; Janson, C. A.; Smith, W. W.; Welsh, K.; Freer, S. Stereochemical mechanism of action for thymidylate synthase based on the X-ray structure of the covalent inhibitory ternary complex with 5-fluoro-2′-deoxyuridylate and 5,10-methylenetetrahydrofolate. *J. Mol. Biol.* **1990**, *214*, 937−948.
(12) Schiffer, C. A.; Clifton, I. J.; Davisson, V. J.; Santi, D. V.; Stroud, R. M. Crystal Structure of Human thymidylate synthase: a structural mechanism for guiding substrate into the active site. *Biochemistry* **1995**, *34*, 16279−16287.
(13) Kuntz, I. D. Structure-Based Strategies for Drug Design and Discovery. *Science* **1992**, *257*, 1078−1082.
(14) Bohacek, R. S.; McMartin, C.; Guida, W. C. The art and practice of structure-based drug design - a molecular modeling perspective. *Med. Res. Rev.* **1996**, *16*, 3−50.
(15) Varney, M. D.; Marzoni, G. P.; Palmer, C. L.; Deal, J. G.; Webber, S.; Welsh, K. M.; Bacquet, R. J.; Bartlett, C. A.; Morse, C. A.; Booth, C. L. J.; Herrmann, S. M.; Howland, E. F.; Ward, R. W.; White, J. Crystal-structure-based design and synthesis of benz-[c,d]indole-containing inhibitors of thymidylate synthase. *J. Med. Chem.* **1992**, *35*, 663−676.
(16) Webber, S. E.; Bleckman, T. M.; Attard, J.; Deal, J. G.; Kathardekar, V.; Welsh, K. M.; Webber, S.; Janson, C. A.; Matthews, D. A.; Smith, W. W.; Freer, S. T.; Bacquet, R. J.; Howland, E. F.; Booth, C. L. J.; Ward, R. W.; Hermann, S. M.; White, J.; Morse, C. A.; Bartlett, C. A. Design of Thymidylate Synthase inhibitors using protein crystal structures: the synthesis and biological evaluation of a novel class of 5-substituted quinazolinones. *J. Med. Chem.* **1993**, *36*, 733−746.
(17) Varney, M. D.; Palmer, C. L.; Deal, J. G.; Webber, S.; Welsh, K. M.; Bartlett, C. A.; Morse, C. A.; Ward, W.; Smith, W. W.; Janson, C. A. Synthesis and biological evaluation of novel 2,6-diaminobenz[cd]indole inhibitors of thymidylate synthase using the protein structure as a guide. *J. Med. Chem.* **1995**, *38*, 1892−1903.
(18) Jones, T. R.; Varney, M. D.; Webber, S. E.; Lewis, K. K.; Marzoni, G. P.; Palmer, C. L.; Kathardekar, V.; Welsh, K. M.; Webber, S.; Matthews, D. A.; Appelt, K.; Smith, W. W.; Janson, C. A.; Villafranca, J. E.; Bacquet, R. J.; Howland, E. F.; Bartlett, C. A.; Morse, C. A. Structure-based design of lipophilic quinazoline inhibitors of thymidylate synthase. *J. Med. Chem.* **1996**, *39*, 904−917.
(19) Costi, M. P. Thymidylate synthase inhibition: A structure-based rationale for drug design. *Med. Res. Rev.* **1998**, *18*, 21−42.
(20) Pendergast, W.; Dickerson, S. H.; Johnson, J. V.; Dev, I. K.; Ferone, R.; Duch, D. S.; Smith, G. H. Benzoquinazoline inhibitors of thymidylate synthase: enzyme inhibitory activity and cytotoxicity of some sulfonamidobenzoylglutamate and related derivatives. *J. Med. Chem.* **1993**, *36*, 3464−3471.
(21) Varney, M. D.; Palmer, C. L.; Deal, J. G. (Agouron Pharmaceuticals, Inc.) PCT Int. Appl. WO96 02, 502 (C1. C07D209/62), Feb 1, 1996; U.S. Appl. 276,929, July 19, 1994; 44 pp.
(22) Gangjee, A.; Mavandadi, F.; Kisliuk, L.; McGuire, J. J.; Queener, S. F. 2-Amino-4-oxo-5-substituted-pyrrolo[2,3-d]pyrimidines as nonclassical antifolate inhibitors of Thymidylate Synthase. *J. Med. Chem.* **1996**, *39*, 4563−4568.
(23) Jones, T. R.; Webber, S. E.; Varney, D. M.; Lewis, K. K.; Kathardekar, V.; Mazdiyasni, H.; Deal, J.; Nguyen, D.; Welsh, K. M.; Webber, S.; Johnston, A.; Matthews, D. A.; Janson, C. A.; Bacquet, R. J. H.; Howland, F. E.; Booth, C. L. J.; Herrman, S. M.; Ward, R. W.; White, J.; Bartlett, C. A.; Morse, C. A. Structure-based design of substituted diphenyl sulfones and sulfoxides as lipophilic inhibitors of thymidylate synthase. *J. Med. Chem.* **1997**, *40*, 677−683.
(24) Jackman, A. L.; Kimbell, R.; Brown, M.; Brunton, L.; Boyle, F. T. Quinazoline thymidylate synthase inhibitors: methods for assessing the contribution of polyglutamation to their in vitro activity. *Anticancer Drug Des.* **1995**, *10*, 555−572.
(25) Gangjee, A.; Vasudevan, A.; Kisliuk, R. L. Nonclassical 5-Substituted Tetrahydroquinazolines as Potential Inhibitors of Thymidylate Synthase. *J. Heterocycl. Chem.* **1997**, *34*, 1669−1676.
(26) Shoichet, B. K.; Stroud, R. M.; Santi, D., V.; Kuntz, I. D.; Perry, K. M. Structure-based discovery of inhibitors of thymidylate synthase. *Science* **1993**, *259*, 1445−1450.
(27) Stout, T.; Tondi, D.; Rinaldi, M.; Barlocco, D.; Pecorari, P.; Santi, D. V.; Kuntz, I. D.; Stroud, R. M.; Shoichet, B. K.; Costi, M. P. Structure-Based Design of Inhibitors Specific for bacterial Thymidylate Synthase. *Biochemistry* **1999**, *38*, 1607−1617.
(28) Hubacher, M. H. The phthaleins from phenol and 1,2-naphthalenedicaroxylic acid. *J. Am. Chem. Soc.* **1944**, *66*, 255−256.
(29) Waley, S. G. A Quick Method for the Determination of Inhibition Constants. *Biochem. J.* **1982**, *205*, 631−633.
(30) Scott, G. W.; Blasquez, J.; Baquero, F.; Shoichet, B. K. Structure-Based Enhancement of Boronic Acid Inhibitors of Ape $\beta$-Lactamase. *J. Med. Chem.* **1998**, *41*, 4577−4586.
(31) Climie, S.; Santi, D. V. Chemical synthesis of the Thymidylate Synthase gene. *Proc. Natl. Acad. Sci. U.S.A.* **1990**, *87*, 633−637.
(32) Kealey, J. T.; Santi, D. V. Purification methods for recombinant Lactobacillus casei thymidylate synthase and mutants: a general, automated procedure. *Protein Expression Purif.* **1992**, *3*, 380−385.
(33) Livi, L. L.; Edman, U.; Schneider, G. P.; Greene, P. J.; Santi, D. V. Cloning, expression and characterization of thymidylate synthase from *Cryptococcus neoformans*. *Gene* **1994**, *150*, 221−226.
(34) Edman, U.; Edman, J. C.; Lundgren, B.; Santi, D. V. Isolation and expression of the *Pneumocystis carinii* Thymidylate Synthase Gene. *Proc. Natl. Acad. Sci. U.S.A.* **1989**, *86*, 6503−6507.
(35) Davisson, V.; Sirawaraporn, W.; Santi, D. V. Expression of Human Thymidylate Synthase in *Escherichia coli*. *J. Biol. Chem.* **1989**, *264*, 9145−9148.
(36) Pogolotti, A. L., Jr.; Danenberg, P. V.; Santi, D. V. Kinetics and mechanism of interaction of 10-propargyl-5,8-dideazafolate with thymidylate synthase. *J. Med. Chem.* **1986**, *29*, 478−482.
(37) Segel, I. H. *Enzyme Kinetics*; John Wiley and Sons, Inc.: New York, 1975; p 173.
(38) Segel, I. H. *Enzyme Kinetics*; John Wiley and Sons, Inc.: New York, 1975; p 105.
(39) Soragni, F.; Costi, M. P. Unpublished.
(40) Pauwels, R.; Balzarini, J.; Baba, M.; Snoeck, R.; Schols, D.; Herdewijn, P.; Desmyter, J.; De Clercq, E. Rapid and automated tetrazolium-based colorimetric assay for the detection of anti-HIV compounds. *J. Virol. Methods* **1988**, *20*, 309−321.
(41) Elion, G. B.; Rideout, J. L.; De Miranda, P.; Collins, P.; Bauer, D. J. Biological activities of some purine arabinosides. *Ann. N. Y. Acad. Sci.* **1975**, *255*, 468−480.

JM9900016